Effect of Backing Plate Thermal Property on Friction Stir Welding of 25-mm-Thick AA6061

PIYUSH UPADHYAY and ANTHONY REYNOLDS

By using backing plates made out of materials with widely varying thermal diffusivity this work seeks to elucidate the effects of the root side thermal boundary condition on weld process variables and resulting joint properties. Welds were made in 25.4-mm-thick AA6061 using ceramic, titanium, steel, and aluminum as backing plate (BP) material. Welds were also made using a "composite backing plate" consisting of longitudinal narrow strip of low diffusivity material at the center and two side plates of high diffusivity aluminum. Stir zone temperature during the welding was measured using two thermocouples spot welded at the core of the probe: one at the midplane height and another near the tip of the probe corresponding to the root of the weld. Steady state midplane probe temperatures for all the BPs used were found to be very similar. Near root peak temperature, however, varied significantly among weld made with different BPs all other things being equal. Whereas the near root and midplane temperature were the same in the case of ceramic backing plate, the root peak temperature was 318 K (45 °C) less than the midplane temperature in the case of aluminum BP. The trends of nugget hardness and grain size in through thickness direction were in agreement with the measured probe temperatures. Hardness and tensile test results show that the use of composite BP results in stronger joint compared to monolithic steel BP.

DOI: 10.1007/s11661-013-2121-0

I. INTRODUCTION AND BACKGROUND

THERMAL boundary condition at the bottom of the work piece is important in determining the weld process response and resulting weld properties. For a given plate geometry, alloy type, and tool design, the choice of weld control parameters (tool rotation speed, welding speed, and forge force), which results in "good" weld, depends on the thermal boundary conditions (BC) at the work piece. The rate of heat flux through the bottom of the work piece mostly depends on the backing plate (BP) diffusivity and hence, as has been pointed out in literature the most important thermal BC for the process is the thermal condition at the BP.[1–3]

Unfortunately, the effects of changes in thermal boundary condition at the bottom of the work piece during friction stir welding have not been thoroughly examined in the open literature. Consequently the effects of thermal management at the bottom of the work piece are poorly understood at present. Rosales *et al.*[4] reported welds made with AA2024 and AA6013 where steel, copper, and ceramic-coated BPs were used at three different combinations of rotational and welding speeds while the forge force was kept constant. The in-plate far field temperature measurements varied significantly when using different BPs indicating the importance of BP conductivity. As a part of quench sensitivity study, Nelson *et al.*[5] reported that the use of heated BP resulted in higher peak temperature and lower cooling rate, yielding inferior mechanical properties in AA7075 welds. Some researchers have used thermal management at the BP to optimize friction stir spot welding (FSSW) process in relatively thin sheets. Su *et al.*[6] for instance reported that in FSSW of 1.3-mm-thick AA 6111 a greater fraction (from 12.5 to 50 pct) of energy generated by the tool was transferred into the weld zone when mica clamp and BP was used instead of conventional steel clamp and BP. This is reasonable since the heat dissipated into the BP is reduced with greater insulation. In a similar study, in FSSW of 0.9-mm-thick AA 6111, Bakavos and Prangnell[7] found that the use of ceramic BP resulted in 318 K (45 °C) increase in the peak processing temperature while lap shear strength was reduced by 15 pct compared to conventional steel BP.

As the application of friction stir welding widens, it will be important to understand the behavior of process variables like stir zone temperature and resulting weld properties with the change in thermal boundary condition. In this paper the authors have focused on the role of BP material on resulting weld properties for 25.4-mm-thick AA 6061. The relatively thick plate allows for greater resolution of weld properties. Nugget grain size and hardness in through thickness direction in the presence of different levels of thermal gradients is presented. Various configurations of BPs and their effect on tensile properties of the weld are also reported.

PIYUSH UPADHYAY, Post-Doctoral Researcher, formerly with the Department of Mechanical Engineering, University of South Carolina, 300 Main Street, Columbia, SC 29208, is now with the Pacific Northwest National Laboratory, Richland, WA. Contact e-mail: piyush.upadhyay@pnnl.gov ANTHONY REYNOLDS, Professor, is with the Department of Mechanical Engineering, University of South Carolina.

Manuscript submitted June 12, 2013.
Article published online November 23, 2013

II. EXPERIMENTAL PROCEDURE

Friction stir welds were made on 25.4-mm-thick rolled plates of the aluminum alloy, AA 6061. Welds were produced on a hydraulically powered MTS FSW process development system (PDS) using *Z*-axis (forge) force control.

The tool used for production of all welds was of a two piece design with a 35 mm diameter, single scroll, H13 tool steel shoulder and a probe fabricated out of MP-159 (a high temperature cobalt based super alloy) in the shape of a truncated cone (8 deg taper) with threads and three flats and 12 mm at the tip. The probe was 25.2 mm long, with a diameter of 19 mm at the intersection with the shoulder. Temperature during welding was recorded using two K-type thermocouples spot welded into the probe, one at the probe midplane height another 0.3 mm above the tip of the probe corresponding to the root of the weld. While the lower thermocouple was situated at the center of the tip, the upper thermocouple was off set midway between the outside surface and tool axis of rotation (see Figure 1).

The experimental conditions used are tabulated in Table I. Preliminary welds (Set#1) were made as bead on plate using four different BPs (each 13 mm thick) with widely varying thermal diffusivity values. Ceramic tile used in the experiment was commercially available floor tile produced by firing plastic clay, sand and feldspar as major raw material. To test the efficacy of composite BP (explained later) and further understand the role of BP welded joints were made using various BP configurations (Set#2 and #3). The applied forge force was obtained from several trial and error runs made with the material. For Set#1 some adjustments in forge force were made such that the weld surface quality and flash condition were similar for all the cases. However for Set# 2 and #3 constant forge forces were used for each BP tested to ensure consistency. Since the welding speed is doubled in Set#2 and #3 slightly larger forces were required. For the last two sets as received T6 temper AA6061 were solution heat treated to T4 state prior to the welding. Samples were extracted from the end of each weld for subsequent characterization.

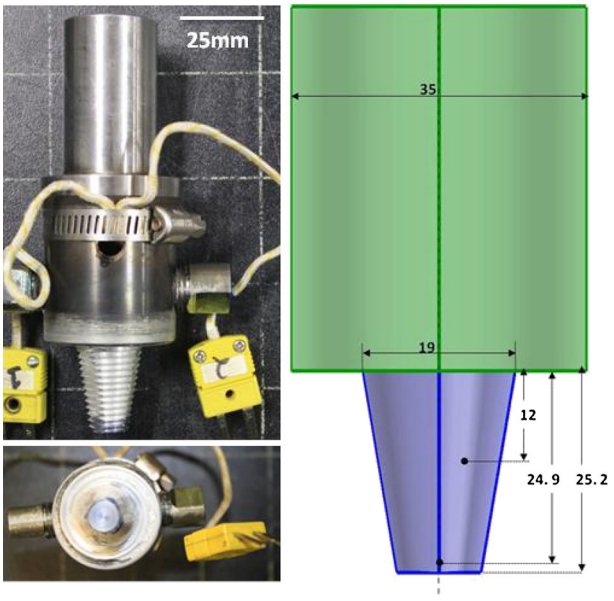

Fig. 1—Left: tool used for the welding. Right: sketch shows the probe and the shoulder only. Black dots indicate the locations of thermocouples. All the dimensions are in mm.

Standard metallographic preparation techniques were employed to grind and polish samples to satisfactory level before performing optical characterization and hardness testing. Samples were ground using automatic and manual grinding machines with 180, 240, 320, 400, 600, 800 grit silicon carbide paper. They were then polished using aluminum oxide powder of 5 and 3 μm size followed by colloidal silica (<0.05 μm). Samples were etched using modified Keller's reagent. Grain sizes were measured at different zones of the nugget using the mean line intercept method.[8] Three views at a magnification of 200× were examined. Grain boundary intersections were counted on a test line of length 0.5 mm (100 mm at 200×).

Microhardness tests were performed using a Vickers hardness indenter on naturally aged and heat treated samples. Post-weld heat treatments of samples were carried out at 433 K (160 °C) for 18 hours. A Vickers hardness indenter, with a load of 500 g and a load application time of 10 seconds was used for measurement of hardness as a function of distance from the weld centerline on transverse cross-sections. Rectangular transverse tensile samples of 178 mm gage length and 12.7 mm width were machined from the welded plate. All the tensile samples were obtained from the portion of the weld where the probe temperature was steady.

III. RESULTS AND DISCUSSION

A. *Weld Temperature*

Figures 2(a) and (b) show the temperature transients recorded by two thermocouples (TC) at midplane and tip of the tool during the welding for two extreme cases of BP *viz*: (a) aluminum and (b) ceramic. Temperature at both the TC locations reaches a reasonable stable state quickly after the plunge sequence. Stable temperature at both the spots in the probe are about the same for ceramic BP while for aluminum BP the near tip tool temperature is significantly lesser than the corresponding midplane probe temperature. Steady state peak temperatures extracted from all the four weld cases with different BPs are presented in Figure 3. The corresponding peak temperatures attained at the indicated spots are plotted against the corresponding thermal diffusivity of the BPs. Indicated alongside the midplane temperature points are the forge forces used during each BP. With some adjustment of forge force, which was needed to maintain similar steady state weld surface quality and flash level, a remarkably similar peak midplane probe temperature of ~755 K (482 °C) was recorded in all of the BP conditions. Root peak temperature however varied significantly among the BPs used. Root peak temperature is same as the midplane T for ceramic BP whereas that for aluminum BP the temperature is 318 K (45 °C) less. This clearly is the effect of BP thermal

Table I. Detail of the Welds Performed on 25.4-mm-Thick AA6061-T6

Set#	Backing Plate, Thickness	RPM	Welding Speed (mm/s)	Forge Force (kN)	Temper Prior to Weld	Welded Plate Dimension
1	aluminum, 13 mm steel, 13 mm Ti-6Al-4V, 13 mm ceramic, 13 mm	480	3.4	40 35.6 31 31	T6	305 mm × 153 mm
2	(1) steel only, 25 mm (2) steel/aluminum, 25 mm	480	6.8	47	T4	610 mm × 610 mm
3	(1) aluminum only, 25 mm (2) steel/aluminum, 25 mm (3) Ti-6Al-4V/aluminum, 25 mm (4) steel only, 25 mm	480	6.8	51	T4	560 mm × 280 mm

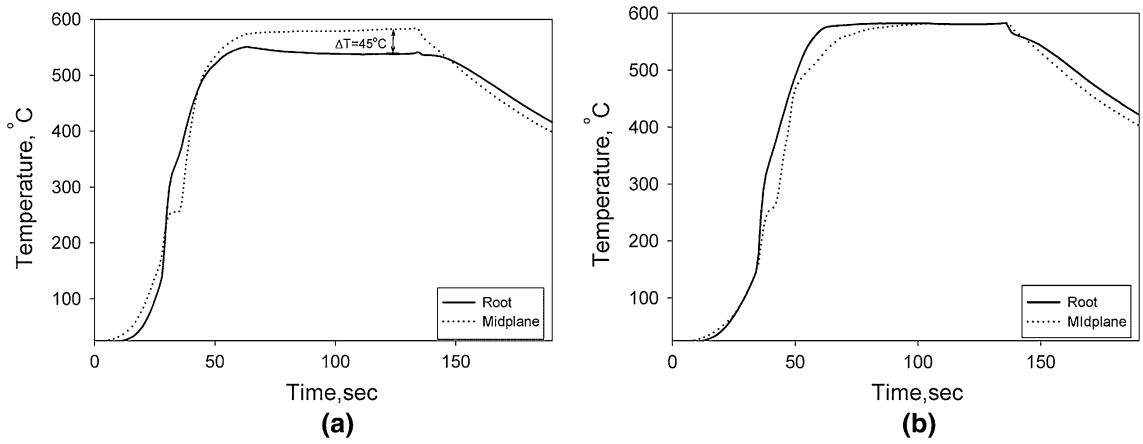

Fig. 2—(*a*) Temperature transients at the two locations of the tool probe for welds made with aluminum backing plate. (*b*) Temperature transients at the two locations of the tool probe for welds made with ceramic tile backing plate.

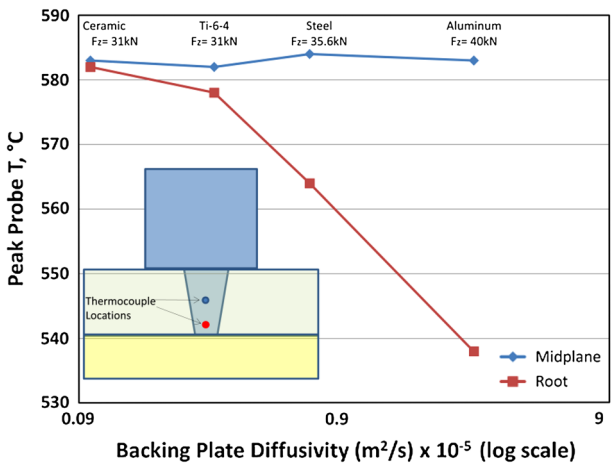

Fig. 3—Measured peak T at two indicated locations in the probe plotted against the thermal diffusivity of the backing plates used. Sketch on the lower left corner of the graph shows the approximate locations of thermocouples within the tool.

condition and shows that the effect of BP diffusivity is highest at the bottom of the work piece. The effect of this through thickness temperature variation is clearly seen in weld properties such as hardness and grain size discussed shortly.

B. *Microstructural Changes in the Nugget*

Figure 4 shows polished and etched transverse cross-section of the weld samples from each of the BPs. The shape and size of the weld nugget for all the cases are similar; however, there are some subtle differences especially at the root region. For instance, the recrystallized nugget for all the cases except Al BP runs down to the bottom edge of the plate. For Al BP the boundary of the recrystallized area is ~0.8 mm above the bottom edge. Also at the root region the width of the thermo-mechanically affected zone (TMAZ) etched as dark band on the both sides of the nugget appear to gradually increase with the increase in diffusivity of the BP. This might indicate that a greater volume of material is engaged with ceramic tile BP compared to Al BP.

The effect of varying degree of through thickness thermal gradients with welds done in otherwise identical conditions can be further illustrated by analyzing the nugget grain size. Although clear relationship between peak temperature during processing and resulting grain size has not been properly established, several researchers have shown that the nugget grain size increases with the increase in the peak temperature.[9–11]

Representative nugget grain microstructure near the crown, midplane, and root is shown for welds made using three cases of BPs in Figure 5. The applied forge

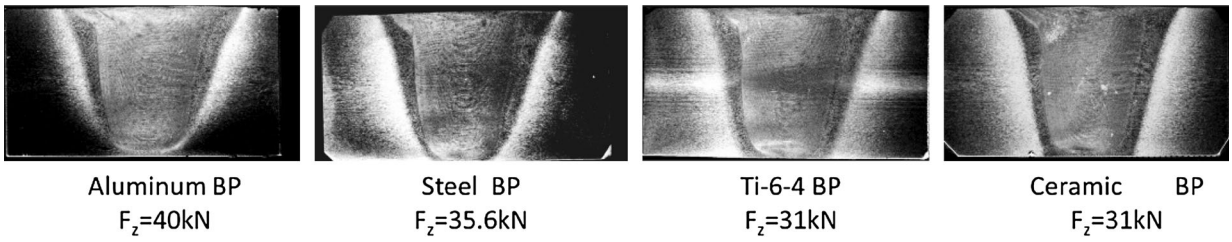

Fig. 4—Transverse etched cross-section of welded samples. Backing plates and forge force used in each case is indicated.

force and peak temperature achieved at tool midplane and tip (near root) are also indicated. Also indicated are the average grain size measured using mean line intercept methods from the respective micrograph. The indicated errors are based on standard deviation of 5 measurements for each case. Such measured grain sizes for all the four cases of BPs are shown in the form of bar chart in Figure 6. Referring to these two figures, grain sizes among all the four BPs are very close to each other (~12.5 μm) at the nugget midplane. Near root grain size on the other hand, vary significantly among different BPs and can be related to the peak temperature attained at the root. Whereas for insulating ceramic BP the grain size at the root and midplane are about the same, for Al BP the grain size at the root is half of that at the midplane. All of the above observations indicates that nugget grain sizes at both the locations are directly relatable to measured tool temperature. Since near crown temperature was not measured, the correlation of peak T with near crown nugget size cannot be made. Interestingly, for most of the cases the near crown grain sizes are slightly smaller than midplane ones. This might suggest that the peak temperature near the crown is lesser than that at the midplane.

C. *Microhardness Results and Correlations*

Figure 7 shows both naturally aged (30 days) and post-weld heat treated (PWHT) transverse hardness profiles for the welds made using two extreme BP materials: aluminum and ceramic tile. Post-weld heat treatment was done at time and temperature, which resulted in T6 temper as mentioned in the experimental section.

With the exception of near root region in the case of aluminum BP weld, there is a substantial increase in nugget hardness after heat treatment: an increase of 25 to 30 VHN can be seen. Strength increase in the HAZ on the other hand is only marginal. Recovery in hardness after heat treatment mainly depends on the amount of solute that is available in the matrix for re-precipitation into strengthening type precipitates.[12–16] Whereas the nugget underwent a high temperature cycle leading to solutionizing of all the phases, the HAZ peak temperature is significantly lower [~623 K (350 °C)]—a temperature known to favor precipitate coarsening thus depleting solute available for re-precipitation during subsequent heat treatment. This deficit in solute in the HAZ causes only marginal strength recovery in HAZ compared in the nugget.

This is because of the relatively small amount of solute being available at the HAZ for the precipitation of strengthening phase compared to the nugget where temperature is greater than solution temperature leading to sufficient precipitation of strengthening phases.[9,17]

The PWHT average nugget and HAZ minimum hardness values obtained from hardness profiles including those shown in Figure 7 are presented in Figures 8(a) and (b) respectively. With ceramic and steel BPs the average nugget hardness near the crown, midplane, and root regions, all fall within 100 to 105 HV, very close to T6 base-metal value of 110 HV. In other words, the nugget almost regains the base material hardness. Also there is essentially no difference in hardness from crown to root for these two cases of BPs. Although the measured temperature for Steel BP is ~293 K (20 °C) less than that of ceramic BP near the root, the average nugget hardness in both the cases are similar. This probably has to do with the fact that both the peak Ts are well beyond the solution heat treatment temperature (SHT) of 802 K (529 °C). At a temperature beyond the solution treatment temperature all the solutes are available for re-precipitation into strengthening precipitate during post-weld aging thus resulting in peak strength. With aluminum BP on the other hand there is a large drop in hardness from value of 100 HV at the midplane to 80 HV near the root. This decrease in hardness can be explained by the observed lower peak T of 811 K (538 °C) in this region as seen in Figures 2(a) and 3. Apparently the region did not attain full solution heat treatment, thus lesser amount of solute were available for re-precipitation into strengthening precipitates during post-weld aging. This result is very similar to the previous grain size results showing direct correlation to the measured temperature.

Although the nugget hardness and its correlation to peak T are interesting, it is the HAZ region that is the weakest link in precipitation hardening alloy. Thus, the HAZ minimum hardness typically determines the joint strength. Considering Figure 8(b), the HAZ minimum hardness with aluminum BP is higher than that with steel and ceramic tile BP. This can be attributed to increased cooling rate in the case of aluminum BP.

D. *Composite Backing Plate Welds and Results*

The results in previous section clearly show that for the considered gage, through thickness homogeneity in temperature, microstructure and hardness can be enhanced by the use of low diffusivity BP. However this

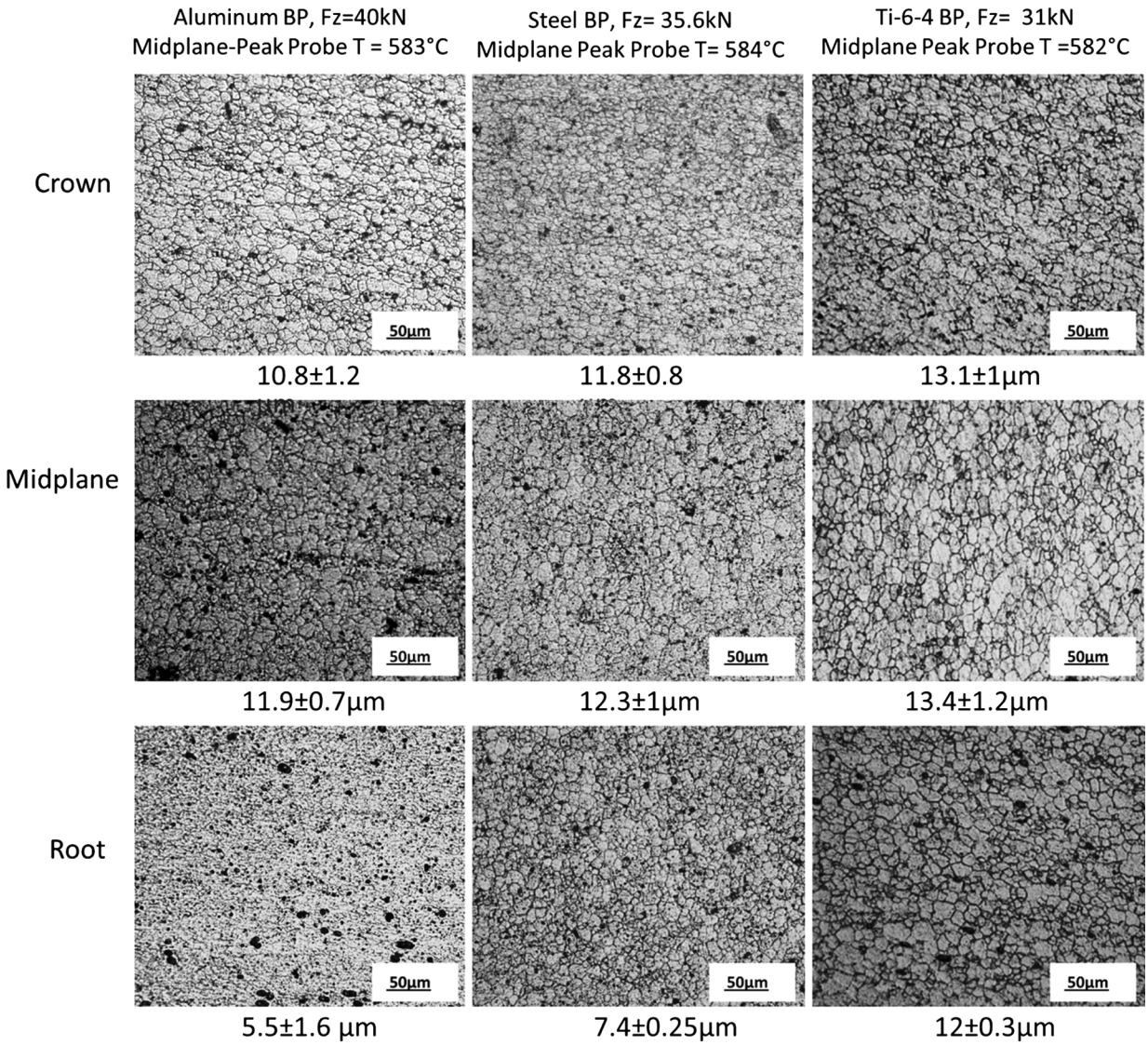

Fig. 5—Representative microstructure showing grain size variations in the nugget at different thicknesses for welds made using aluminum, steel, and Ti-6Al-4V backing plates in 25.4-mm-thick AA6061 at 480 rpm and 3.4 mm/s. The peak temperature measured a the probe midplane for both the cases are similar: ~855 K (582 °C). The measured average grain sizes are indicated.

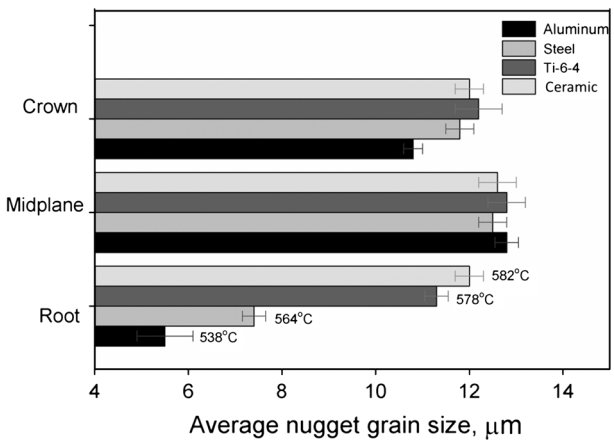

Fig. 6—Average nugget grain size variations at different regions of the welds using different backing plates.

may lead to an unwanted effect; the rate of cooling (quench rate) at the wake of the tool after the weld will be reduced due to insulation at the BP. This might reduce the strength attained after subsequent post-weld aging. This is specifically problematic at the HAZ for precipitation hardening alloys. Use of a composite BP is proposed to circumvent this tradeoff. The schematic of the composite BP is shown in Figure 9. The idea is to use a low diffusivity central strip about the size of the tip of the tool and a high diffusivity backing bar for the outer region. The low diffusivity strip just under the nugget will help insulate the heat escaping from the work piece and is expected to enhance through thickness homogeneity. The side bars being made out of high diffusivity material on the other hand will enhance the heat extraction rate, thus decreasing the time at temperature for precipitate coarsening hence improving the HAZ minimum hardness. Figure 10 shows one of the

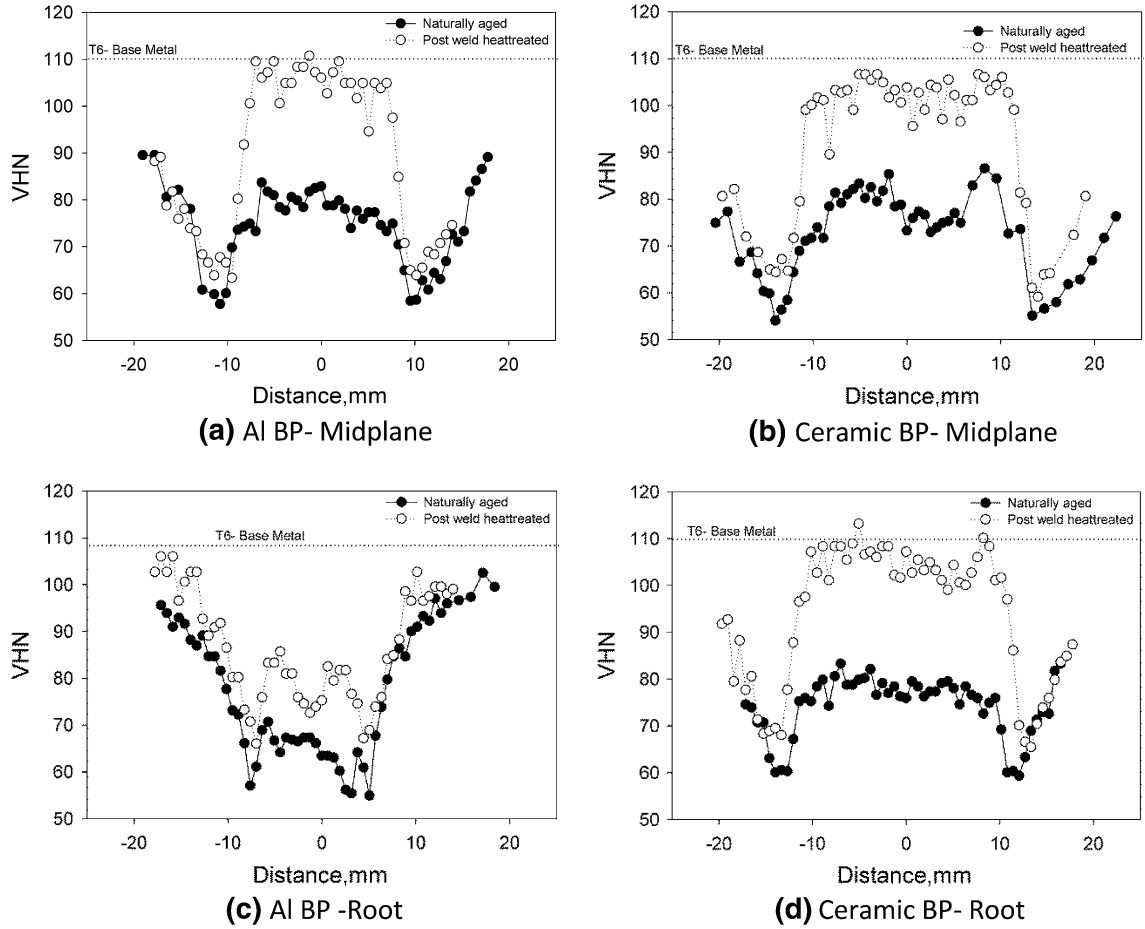

Fig. 7—Naturally aged and PWHT hardness traverses at midplane and near root sections for two extreme cases of backing plates.

assembled composite BP and the weld setup. The goal of this set of experiment was to compare the tensile strength of welded joints made using different BP configuration keeping everything else constant. In order to maximize the strength values a higher welding speed of 6.8 mm/s (twice than what was reported in previous section) was used. Metallographic results obtained from composite BPs and equivalent conventional steel BPs are discussed below.

Figure 11 shows the hardness traverses measured at three regions of the welds made with (a) monolithic steel BP and (b) composite BP consisting of steel central strip and AA6061 as side backing bars. The welding conditions and parameters sets were otherwise identical among the two cases: 480 rpm to 6.8 mm/s and forge force = 47 kN. Note that this speed is twice the speed used in earlier section. The work pieces used for this study were solution heat treated at 803 K (530 °C) into a T4 state prior to welding. This is also different than previously presented cases where the initial temper of the work piece was T6. As indicated in the legend of the figure the steady state peak probe T of the tool at the midplane are similar among steel and composite BP. Near root temperature in composite BP is ~10 K (−263 °C) (not a large difference) lower than that with steel BP most likely owing to greater heat transfer with high diffusivity aluminum side bars. Note that with composite BP the hardness traverses are much more close to each other at different thickness levels suggesting better homogeneity in the hardness. In Figure 12 the average hardness at nugget (a) and HAZ minimum (b) for different regions are shown. The nugget hardness at the midplane and the root regions can be reasonably correlated to the measured peak T just like previous results. Higher nugget hardness in steel BP compared to composite BP is probably due to high level of solution heat treatment because of higher temperature exposure. Most strikingly, the HAZ minimum hardness in the case of composite BP near the root region is substantially greater than that with monolithic steel BP. See Figure 13 where the near root hardness for the two BP conditions are plotted together (18 VHN greater in advancing side and 10 VHN greater in the retreating side).This increase can be decidedly attributed to better cooling rate at the HAZ with aluminum side backing bar. The concept of composite BP has also proven useful to prevent tool marks and indentation, and undesired lap weld at the BP which often occurs when monolithic aluminum BP is used as BP.

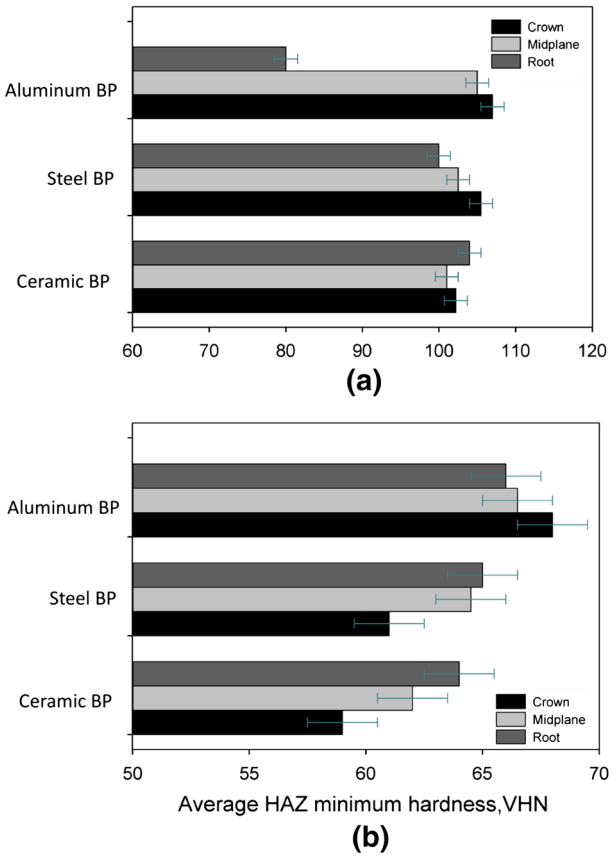

Fig. 8—(*a*) The average nugget hardness values at different regions of the weld shown for three different backing plates. (*b*) The average HAZ minimum hardness values at different regions of the weld shown for three different backing plates.

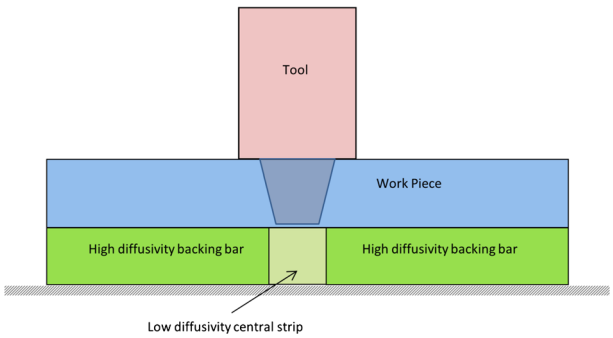

Fig. 9—A block diagram of composite backing plate arrangement.

E. *Tensile Properties*

Encouraged by the hardness results, additional welds (Set#3) were made with the intent of comparing tensile properties of the joints among welds made with different BPs. Four different configurations *viz*: steel only, Ti-6Al-4V/aluminum composite, steel/aluminum composite, and aluminum only BPs were used while all the control parameters were kept constant (details of this set of welds are shown in Table I as Set#3.) Examination of weld cross-section revealed that all the welds in Set#3 contained root side defect caused by lack of tool penetration (LOP). It is to be noted that the LOP defect in situation like this may be avoided by increasing the pin length slightly or reducing the welding speed thus facilitating material flow underneath the probe. Owing to limited time and resources further experiments were not conducted to mitigate LOP defects. Fortunately since the defect was relatively small (maximum length of the defect being less than 1.5 mm in length from the root side, compared to 25.4-mm-thick material) it was possible to completely eliminate the defect from tensile sample without removing significant nugget volume. This was achieved by simply machining 2 mm material off the root of the samples. A total of six samples were tensile tested for each weld run: three full thickness samples with LOP defect and four samples without the LOP defect.

During tensile testing the full thickness samples corresponding to all the BP cases opened up near the root at the location of LOP defect resulting in zigzag fracture line. In the case of samples without LOP defect most of the samples failed along the HAZ region on the retreating side resulting in smooth fracture line. In the case of Steel only BP, however, most of the samples failed at the advancing side edge of the nugget resulting in zigzag fracture line. The quantitative results of tensile testing are discussed below.

Figure 14(a) shows ultimate tensile strength (UTS) in transverse tension values obtained from tensile test performed using full thickness samples consisting of root side LOP defect. Figure 14(b) shows the UTS values obtained from samples with LOP defect removed. Error bars correspond to standard deviation of three tests for each case. Considering both the figures it is clear that BP diffusivity has a significant effect on tensile strength of the welded joint. There is a 25 pct increase in the UTS of the joint with the use of aluminum instead of conventional steel as BP material. Both the composite BPs also show significant strength improvement compared to the steel BP. The aluminum only BP shows marginally better tensile strength compared to two types of composite BP. This likely is the result of greater heat dissipation from the bottom of the work piece. The difference among the three cases, however, is not much. Nevertheless, the result corroborates well with the hardness data shown in Figures 11, 12, and 13 which showed significant difference in HAZ minimum hardness with the composite BPs. It is also interesting to note that there is virtually no difference between the tensile strength of welds with and without the lack of penetration defect. This suggests that a small amount of LOP defect does not pose a threat for static loading cases. In the case of dynamic loading however the early crack initiation at the LOP site will most likely result in poor fatigue property of the joint. This suggests that a small amount of LOP defect does not affect the static tensile property of the joint. However the presence of LOP defect will most likely have significant effect during dynamic loading. Fatigue life of samples with LOP for instance will probably be reduced because of early formation of fracture along the LOP line.

Figure 15 shows the percentage elongation at fracture obtained from the tensile tests. The weld made with aluminum BP has clearly the greatest elongation. The composite BP elongation data falls in between the two

Fig. 10—Picture of composite backing plate (left). Weld setup with composite backing plate (right).

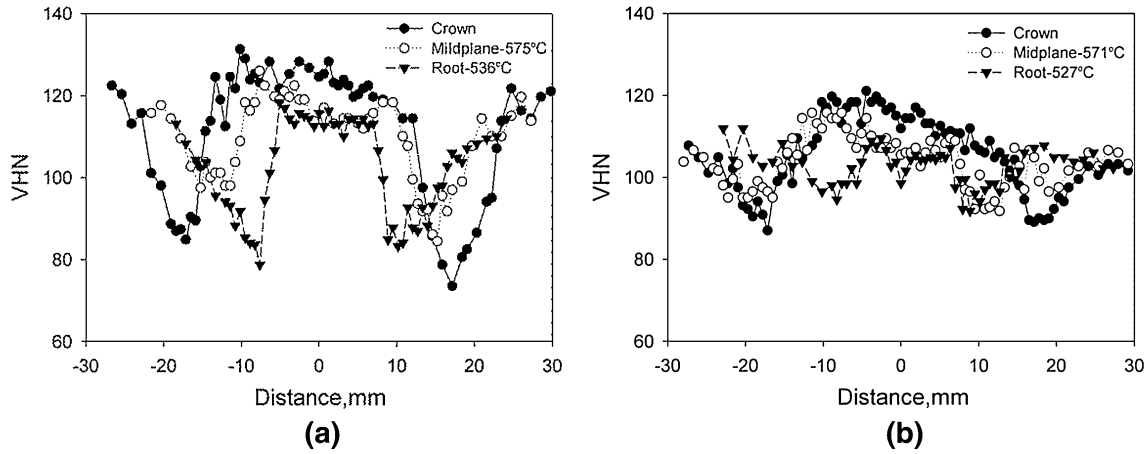

Fig. 11—PWHT hardness traverses at different regions of weld cross-sections for welds made with monolithic and composite backing plates. Peak temperature measured at tool tip and midplane are indicated in the legend. Welds performed at 480 rpm to 6.8 mm/s. Initial temper T4. Post-weld heat treated to T6.

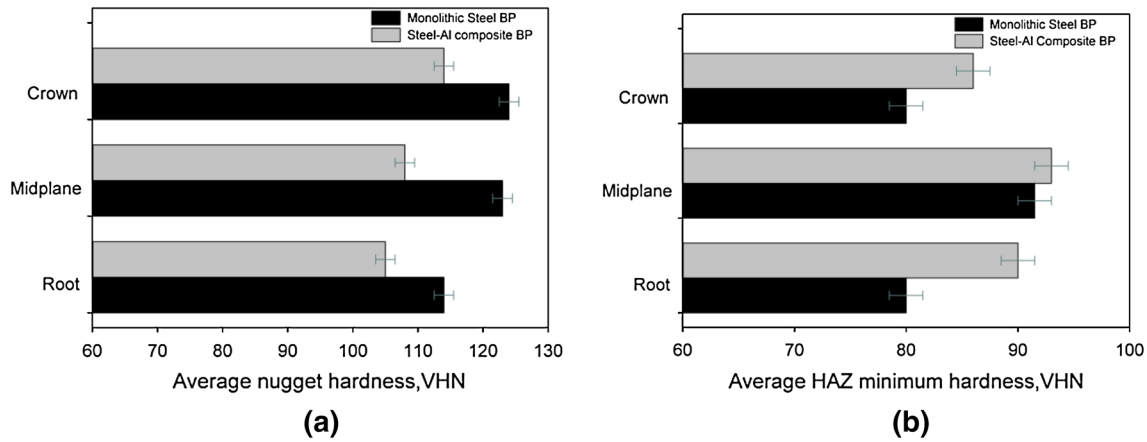

Fig. 12—PWHT average hardness values at the nugget (*a*) and HAZ minimum (*b*) measured at different regions of the weld made with composite and monolithic backing plates for AA6061, all other things being equal. Temper prior to weld: T4. PWHT to T6.

extremes. It is important to point out that although joint elongation values can be useful they are not the measure of the ductility of various regions of the weld. The elongation data obtained from a sample composed of regions with different strengths directly depends on the strength of the region at which strain localization occurred for each case. The elongation results can be explained by relative microhardness distribution at the nugget and HAZ region. In Figure 16 the percentage elongation is plotted against the difference between root side average nugget and HAZ minimum hardness (denoted by ΔHV) for different BP configurations. As the average ΔHV increases more strain is concentrated at the smaller region of HAZ compared to larger nugget area resulting in lesser overall elongation value.

F. *Summary and Conclusions*

The effects of BP thermal property on the resulting process response and mechanical properties were

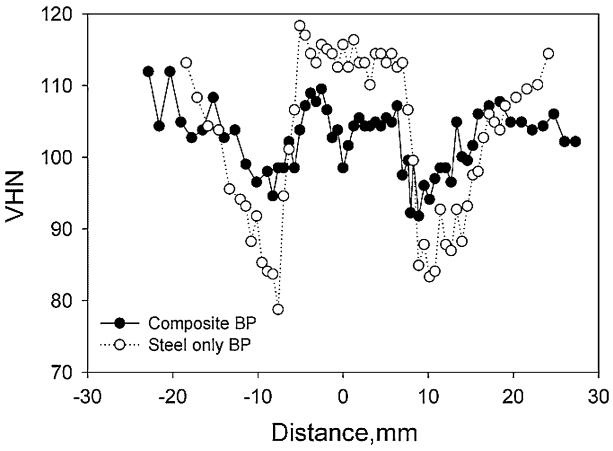

Fig. 13—Comparison of near root PWHT hardness traverses between composite and monolithic backing plates. Temper prior to weld: T4. PWHT to T6.

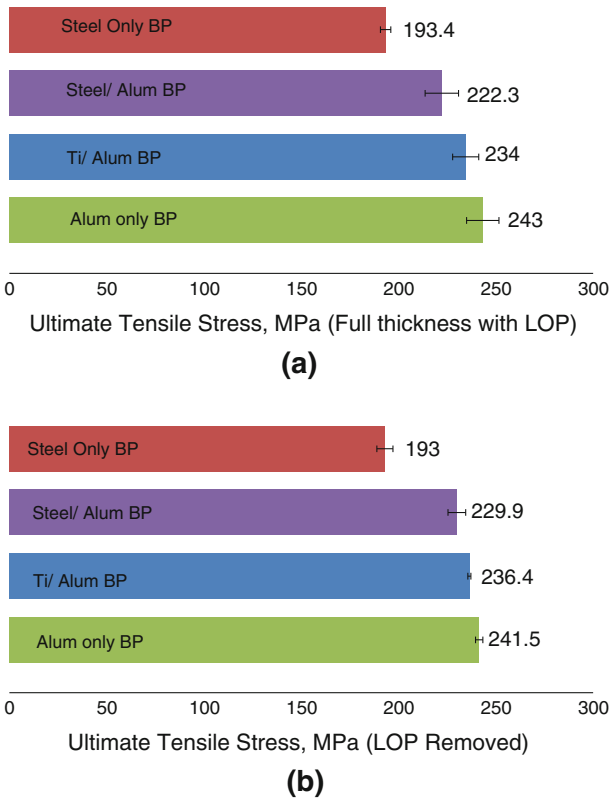

Fig. 14—(*a*) Ultimate tensile strength corresponding to full thickness samples. Temper prior to weld: T4. PWHT to T6. (*b*) Ultimate tensile strength corresponding to samples with LOP defect removed temper prior to weld: T4. PWHT to T6.

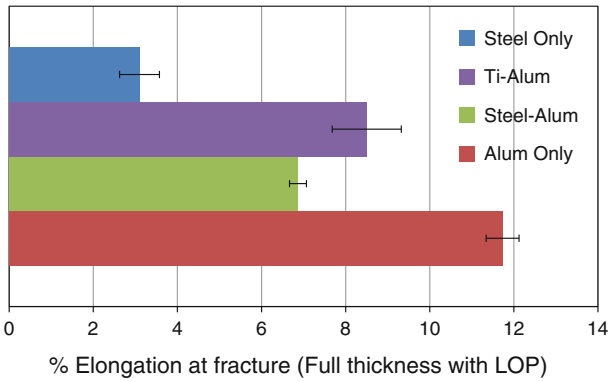

Fig. 15—Percentage elongation corresponding to full thickness samples. Temper prior to weld: T4. PWHT to T6.

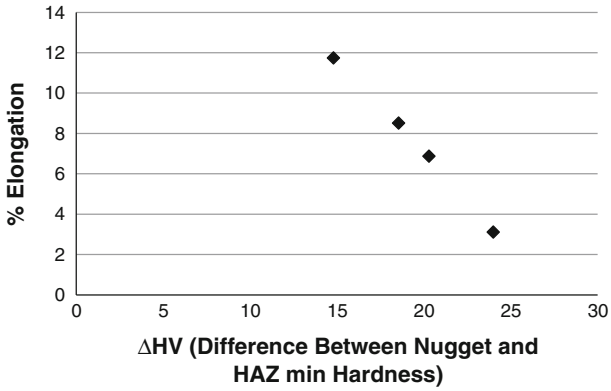

Fig. 16—Pct Elongation Plotted against the difference between nugget and HAZ minimum hardness near corresponding weld roots.

evaluated for friction stir welds made with 25.4-mm-thick AA6061. Temperature measured at two locations in the tool probe showed that the BP thermal diffusivity has a significant effect on through thickness peak temperature distribution in the nugget. Compared to conventional steel BP, peak temperature can be homogenized along the through thickness direction by the use of low diffusivity BP. As a result of homogeneous temperature, the weld property in the nugget *viz*. grain size and hardness were homogenized with the use of low diffusivity BP (Ti-6Al-4V and ceramic) compared to conventional steel BP. Use of composite BP consisting of low diffusivity central strip and side bars of aluminum has produced promising results. Both transverse microhardness and tensile tests show that aluminum only and two different configurations of composite BP resulted in stronger weld joints compared to weld made using monolithic steel BP.

ACKNOWLEDGMENTS

The authors acknowledge the financial support of the Center for Friction Stir Processing which is a National Science Foundation I/UCRC supported by Grant No. EEC-0437341. The authors thank Dr. Wei Tang and Daniel Wilhelm, Department of Mechanical Engineering, University of South Carolina, Columbia, SC, USA for their help in preparing the weld joints.

REFERENCES

1. M.Z.H. Khandkar, J.A. Khan, and A.P. Reynolds: *Sci. Technol. Weld. Join.*, 2003, vol. 8, pp. 165–74.
2. P.A. Colegrove, H.R. Shercliff, and R. Zettler: *Sci. Technol. Weld. Join.*, 2007, vol. 12, pp. 284–97.
3. H. Schmidt: Ph.D. Thesis, Department of Manufacturing Engineering and Management, DTU, Denmark, 2004.
4. M.J.C. Rosales, N.G. Alcantara, J. Santos, and R. Zettler: *MSF.*, 2010, vols. 636–637, pp. 459–64.
5. T.W. Nelson, R.J. Steel, and W.J. Arbegast: *Sci. Technol. Weld. Join.*, 2003, vol. 8 (4), pp. 283–88.
6. P. Su, A. Gerlich, T.H. North, and G.J. Bendzsak: *Sci. Technol. Weld. Join.*, 2006, vol. 11 (2), pp. 163–69.
7. D. Bakavos and P.B. Prangnell: *Sci. Technol. Weld. Join.*, 2009, vol. 14 (5), pp. 443–56.
8. E112-10 Standard Test Methods for Determining Average Grain Size: *Annual Book of ASTM Standards*, vol. 313, ASTM, 2007.
9. Y.S. Sato, M. Urata, and H. Kokawa: *Metall. Mater. Trans. A*, 2002, vol. 33 (3), pp. 625–35.
10. J. Yan, M.A. Sutton, and A.P. Reynolds: *Sci. Technol. Weld. Join.*, 2005, vol. 10 (6), pp. 725–36.
11. K.A.A. Hassan, P.B. Prangnell, A.F. Norman, D.A. Price, and S.W. Williams: *Sci. Tech. Weld. Join.*, 2003, vol. 8 (4), pp. 257–68.
12. A. Simar, Y. Bréchet, B. de Meester, A. Denquin, C. Gallais, and T. Pardoen: *Prog. Mater Sci.*, 2012, vol. 57 (1), pp. 95–183.
13. C. Gallais, A. Denquin, Y. Bréchet, and G. Lapasset: *Mater. Sci. Eng. A*, 2008, vol. 496 (1–2), pp. 77–89.
14. G.A. Edwards, K. Stiller, G.L. Dunlop, and M.J. Couper: *Acta Mater.*, 1998, vol. 46 (11), pp. 3893–904.
15. L.-E. Svensson, L. Karlsson, H. Larsson, B. Karlsson, M. Fazzini, and J. Karlsson: *Sci. Tech. Weld. Join.*, 2000, vol. 5 (5), pp. 285–96.
16. D. Bakavos, P.B. Pragnell, and R. Dif: *Mater. Forum Inst. Mater. Eng.*, 2004, vol. 28, pp. 124–31.
17. R.Y. Hwang and C.P. Chou: *Scripta Mater.*, 1997, vol. 38 (2), pp. 215–21.